Effects of symmetry reduction in two-dimensional square and triangular lattices

T. Trifonov, L. F. Marsal,[1,*] A. Rodríguez,[2] J. Pallarès,[1] and R. Alcubilla[2]
[1]*Departament d'Enginyeria Electrònica, Elèctrica i Automàtica, ETSE, Campus Sescelades, Universitat Rovira i Virgili, Avda. Països Catalans 26, 43007 Tarragona, Spain*
[2]*Departament d'Enginyeria Electrònica, Universitat Politècnica de Catalunya, Edifici C4, Campus Nord, c/ Jordi Girona 1-3, 08034 Barcelona, Spain*
(Received 29 January 2004; published 29 June 2004)

We investigate the absolute photonic band gap (PBG) formation in two-dimensional (2-D) photonic crystals designed using symmetry reduction approach. The lattice symmetry, shape and orientation of dielectric scatterers affect the photonic gap parameters. We use symmetry reduction, achieved either by including additional rods into the lattice unit cell or by reorienting noncircular scatterers to engineer the photonic band gaps in 2-D square and triangular structures. The case of air rods drilled into silicon background is considered. We show that for square structures symmetry reduction can be an effective way to enlarge the absolute PBG, but for triangular lattices any modification of the crystal structure considerably reduces the absolute PBG width. We also discuss the practical technological feasibility of the proposed structures.

DOI: 10.1103/PhysRevB.69.235112 PACS number(s): 78.20.Bh, 42.70.Qs, 41.90.+e

I. INTRODUCTION

Photonic crystals (PCs) are periodic structures in one or more spatial directions. They have received much interest because they offer a way to control and manipulate light. Many unusual optical properties of these photonic crystals have been predicted and some of them have been confirmed experimentally, e.g., the existence of a photonic band gap (PBG), i.e., a frequency range for which light propagation is forbidden inside the structure,[1] the suppression of spontaneous emission[2,3] and the possibility of creating localized defect modes in the photonic band gap.[4,5] However, the fabrication of useful three-dimensional (3-D) photonic crystals in the visible and near IR spectra is a difficult task because of technological limitations at submicrometer length scales. The search for photonic crystals that exhibit larger band gaps and are suitable for the fabrication is still an important issue.

Two-dimensional photonic crystals are easier to fabricate than 3-D ones, especially for the technologically important near IR spectrum. For a 2-D photonic crystal, the electromagnetic wave can be decomposed in two polarization modes: TE modes when the magnetic field is polarized along the rods and TM modes when the electric field is polarized along the rods. An absolute PBG emerges from the overlap between the band gaps for both polarization modes. Several methods have been suggested for optimizing this overlap and thus obtaining the largest possible absolute PBG. As suggested in Ref. 6, for example, introducing anisotropy into one of the dielectric media in a photonic crystal can produce larger absolute photonic band gaps in 2-D square and triangular lattices. However, this method is limited by the availability of the material. Other methods are based on symmetry reduction. Symmetry plays an important role in opening the absolute PBGs.[7] Often, restrictions to the absolute PBG formation are due to the symmetry-induced degeneracies of photonic bands at high symmetry points in the Brillouin zone. The approach therefore involves reducing the structural symmetry to lift these band degeneracies and so enlarge the photonic band gap. Anderson and Giapis[8,9] have shown that inserting small circular rods into the square, honeycomb and group 4*mm* photonic structures reduces the symmetry of the original lattice, thus leading to a larger absolute PBG. These authors have considered only photonic crystals of circular rods. Symmetry reduction can also be achieved by using noncircular scatterers. To introduce asymmetry, Villeneuve and Piche[10] used oval rods instead of circular ones in a triangular lattice but failed to create larger absolute PBG. However, in a rectangular lattice of oval rods, symmetry reduction has been successfully explored to increase the overlapping PBG.[11] Padjen *et al.*[12] studied the triangular lattice of rods with square, rectangular and triangular profiles. They concluded that the circular rod profile leads to the largest absolute PBG but they did not consider the symmetry reduction, achieved by including new elements in the reported structures. Wang *et al.*[13] and more recently Marsal *et al.*[14] have shown that rotating square rods in a square lattice can significantly change the position and size of band gaps for both polarization modes and even increase the overlap between these two gaps. They found that the largest PBG appears when the rotation of square rods is combined with the inclusion of an additional rod in the lattice unit cell.

In short, several studies have already reported the symmetry reduction approach. However, it is difficult to compare the results of these studies because the dielectric contrasts and accuracies used in the calculations were different. Moreover, most of the reported structures are difficult to fabricate because absolute PBG improves when the dielectric walls are extremely thin. As our group works on the fabrication of 2-D photonic crystals based on air/silicon structures, we think that a more detailed examination of such structures that also takes into account the difficulty of fabrication is needed. Our aim in the present study is therefore to analyze the absolute PBG formation for some recently reported structures using silicon with dielectric constant $\varepsilon = 12.096$ as a background material (at wavelength $\lambda = 1.55\ \mu$m[15]). We present numerical simulations of photonic bands for 2-D square and triangular lattices of square and circular air rods drilled in silicon. We also explore their modified structures designed using the

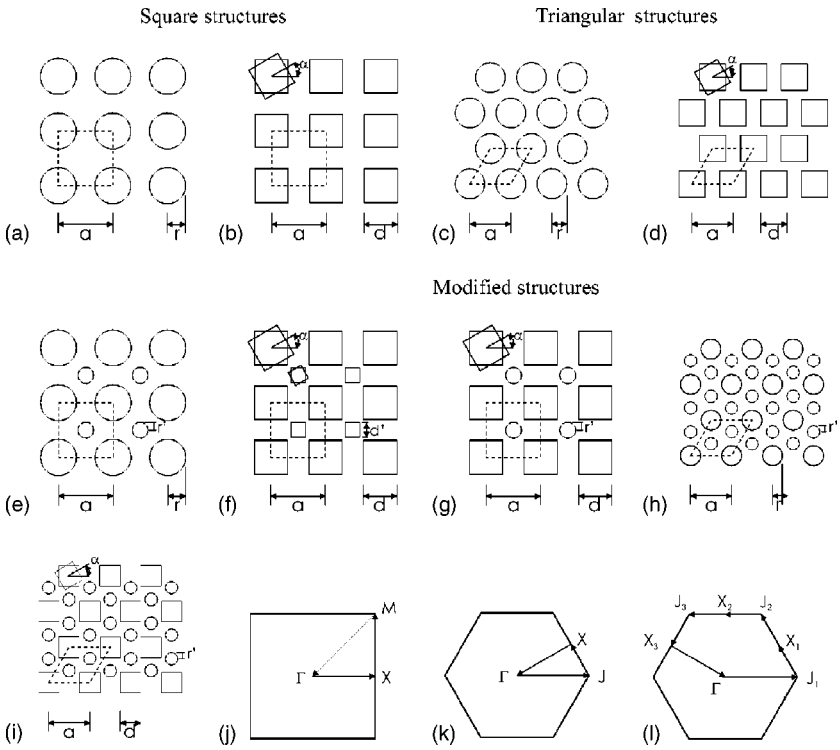

FIG. 1. Patterns of the structures under consideration: (a) square-circles (*lattice-scatterers*); (b) square-squares; (c) triangular-circles; (d) triangular-squares; (e) square-circles with a circular included rod; (f) square-squares with a square included rod; (g) square-squares with a circular included rod; (h) triangular-circles with two circular included rods; (i) triangular-squares with two circular included rods; (j) first Brillouin zone for the square structures; (k) and (l) first Brillouin zone for the triangular structures of circular and square rods, respectively. The lattice unit cell is indicated by a dashed line.

symmetry reduction approach, namely by including additional rods in the basic lattice and by rotating noncircular rods. In our work we focuss on the maximization of the absolute PBG width as a function of crystal parameters and on the technological feasibility of these optimized structures.

II. Lattice description and numerical method

The patterns of 2-D structures under consideration are depicted in Fig. 1, as follows: (a) and (b) basic square lattices of circular and square air rods, respectively; (c) and (d) basic triangular lattices of circular and square air rods; (e), (f) and (g) modified square lattices formed by inclusion of an additional circular or square-shaped rod at the center of the unit cell; (h) and (i) modified triangular lattices formed by the inclusion of two additional circular rods at the middle of each triangle. For brevity, the structures of Figs. 1(a)–1(d) will be referred to as *basic lattices*, while their modified structures [Figs. 1(e)–1(i)] will be referred to as *interstitial lattices*. For all structures the parameters a, d and r denote the lattice constant, the size of basic square rods and the radius of basic circular rods, respectively. The angle of rotation α of square rods is defined as the angle between axes of the square cross section and the lattice axes. The parameters d' and r' denote the size and the radius of the included square and circular rods. For simplicity, the size of the included elements can be related to the size of the basic rods by introducing a new parameter β, which is defined as $\beta = r'/r$ for the interstitial structures in Fig. 1(e) and 1(h); $\beta = d'/d$ for the structure in Fig. 1(f) and $\beta = 2r'/d$ for the interstitial structures in Figs. 1(g) and 1(i). For the case of interstitial lattices, additional degrees of freedom are therefore introduced into the calculations.

The photonic bands of 2-D photonic crystals were calculated using the finite difference time domain (FDTD) method, also known as the *Ordern*(N) method.[16] We assumed that all rods were made of the same material (air with relative dielectric constant $\varepsilon = 1$) and embedded in a background dielectric (silicon with $\varepsilon = 12.096$ at $\lambda = 1.55$ μm). The bands for both polarization modes were calculated: TE modes (H polarization) and TM modes (E polarization). When the square lattices were considered, the Γ, M and X points in the Brillouin zone were included in the calculation [Fig. 1(j)] and the photonic bands were traced along the M-Γ-X-M path. For the triangular lattices of circular rods, the calculations were performed along the J-X-Γ-J path [Fig. 1(k)]. In the case of triangular lattices of square rods, the C_3 rotational symmetry is lifted.[17] However, the rotation of square rods lifts all rotational and mirror symmetries of the lattice. For this reason, the photonic bands were traced along the X_3–Γ-J_1-X_1-J_2-X_2-J_3-X_3 path of the Brillouin zone, as shown in Fig. 1(l). The calculation error was estimated to be less than 2% for frequencies below 1 (in $2\pi c/a$ units).

III. RESULTS AND DISCUSSION

A. Square lattices

We begin our discussion with the basic square structures shown in Figs. 1(a) and 1(b). For the given dielectric contrast, the square structure of circular air rods presents an absolute photonic band gap resulting from the overlap between the TE2-3 (i.e., the gap between the second and the third photonic bands) and the TM3-4 polarization gaps across all symmetry points. This absolute PBG has a maximum normalized width of about $\Delta\omega/\omega_g = 3.4\%$ for $r = 0.492a$. Here, the parameters $\Delta\omega$ and ω_g denote the fre-

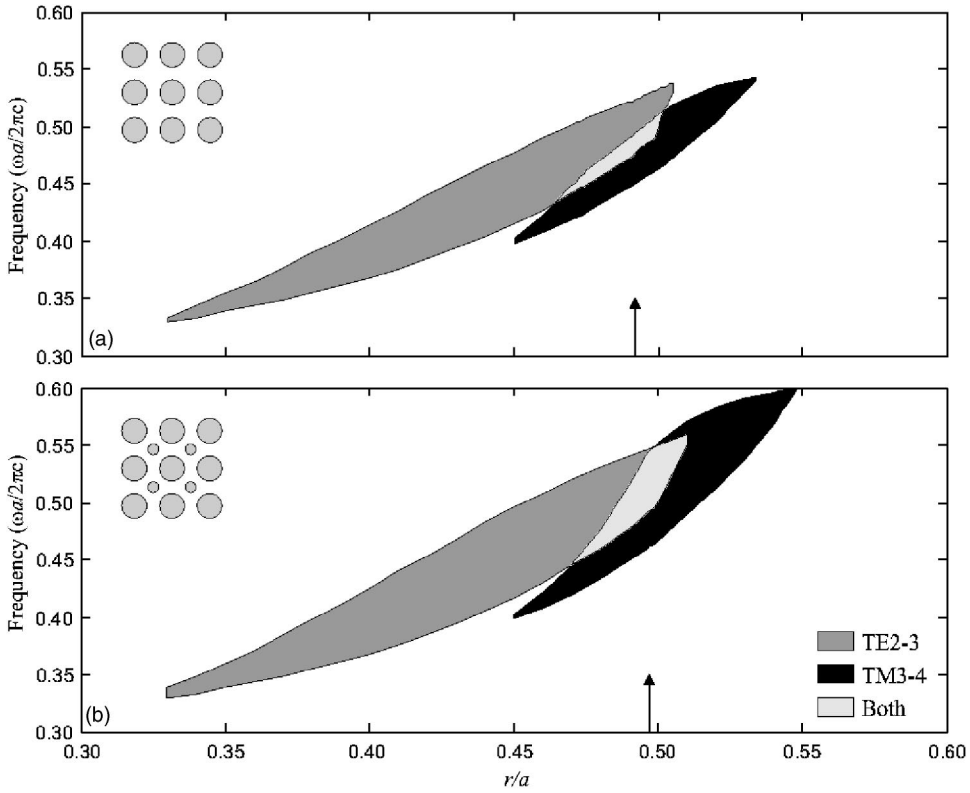

FIG. 2. Photonic gap map for (a) the basic square structure of circular air rods and (b) a modified square structure formed by including an additional circular rod at the center of the unit cell. The figure insets depict the structure under consideration. The positions of maximum absolute PBG width are indicated by arrows.

quency width of the gap and the frequency at the middle of the gap, respectively. In case of square structure with square rod profile, no absolute PBG exists for refractive indexes below 3.51.[18] In particular, this is valid only when the square rods are not rotated. We will demonstrate that the rotation of square rods leads to a larger absolute PBG that extends over a wide range of rod dimensions and rotation angles. The width of the absolute PBG for both basic square structures can be further improved by including additional rod in the lattice unit cell.

In Fig. 2 the dimensionless frequencies of gap boundaries are drawn as functions of r/a for (a) the square lattice of circular rods and (b) its modified lattice with a circular rod included at the center of the unit cell. Here, only TE2-3 and TM3-4 polarization gaps, which form the absolute PBG, are shown. The gap map of the square structure of circular rods [Fig. 2(a)] shows that the maximum width of the absolute PBG appears for rods of radius $r=0.492a$. We can estimate the difficulty of fabrication by centering the gap at wavelength $\lambda=1.55$ μm. In this case, the dielectric walls between air rods should be 10 nm thick. Although this is realistic, it is obviously difficult to fabricate this structure. As can be seen, the TE2-3 polarization gap reduces sharply and closes the absolute PBG as the rod radius nears the close-packed condition $r_{cp}=0.5a$ (i.e., when the rods begin to touch). Band structure analysis shows that second and third TE bands are

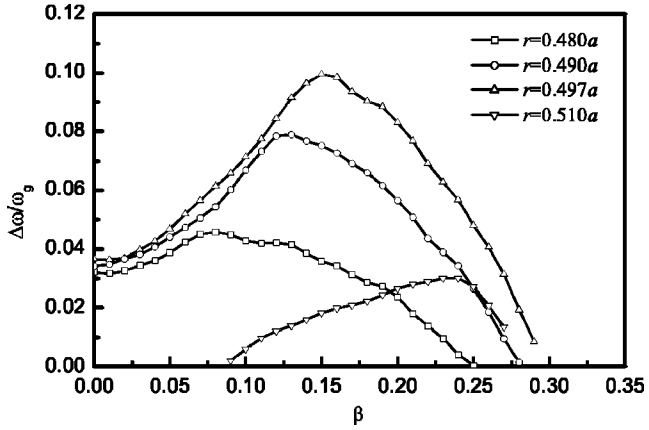

FIG. 3. Dependence of the normalized absolute PBG width ($\Delta\omega/\omega_g$) on the parameter $\beta=r'/r$ for the modified square structure shown in Fig. 1(e) for four different radii r of the basic rods. The maximum absolute PBG appears for $r=0.497a$ and $\beta=0.15$.

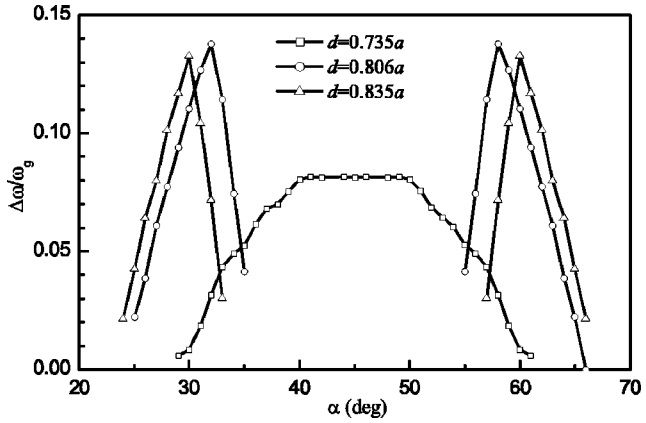

FIG. 4. Dependence of the absolute PBG width ($\Delta\omega/\omega_g$) on the rotation angle α for the square structure of square air rods for different values of square size d. The maximum absolute PBG appears for $d=0.806a$ and $\alpha=32°(58°)$.

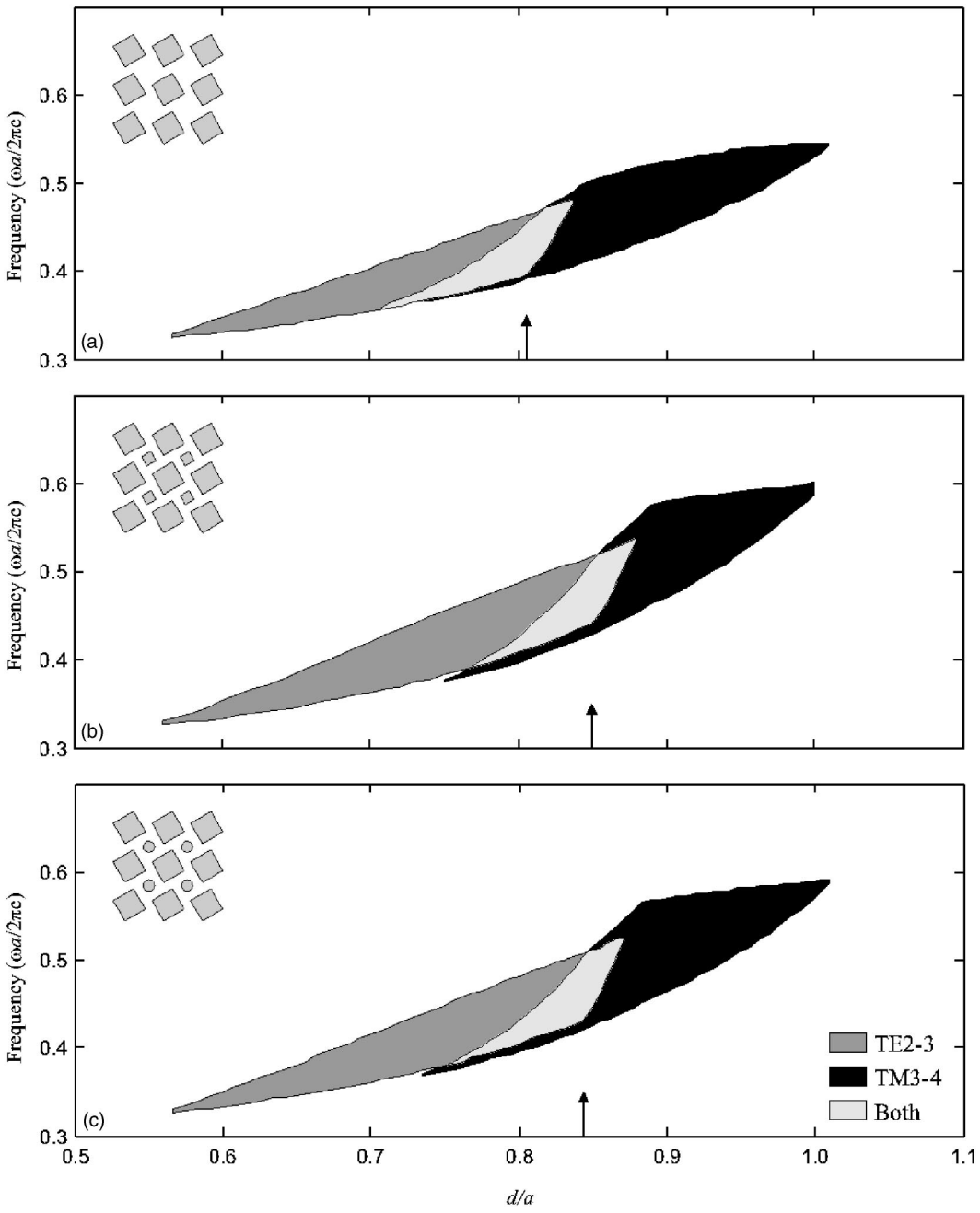

FIG. 5. Positions of TE2-3 and TM3-4 polarization gaps as functions of square length d/a for (a) the square structure of square rods rotated at angle $\alpha=32°$; (b) a modified square structure with a square rod added at the center of the lattice unit cell for $\alpha=27°$ and $\beta=0.15$; (c) a modified structure with a circular rod added at the center of the unit cell for $\alpha=28°$ and $\beta=0.15$. The picture insets show the structures under consideration. The positions of maximum absolute PBG width are indicated by arrows.

degenerate at point **M** of the Brillouin zone. For the modified structure [Fig. 1(e)], this band degeneracy is lifted. The crystal symmetry for this structure is reduced by placing a small rod at the center of each square unit cell. We performed extensive band calculations for different radii of the included rod. Figure 3 shows the normalized width of the absolute band gap as a function of the parameter $\beta=r'/r$, which is the ratio between the radii of the included r' and the basic r rods. The overall tendency is clearly seen: for small values of β the absolute PBG width is greater than in the case without inclusion ($\beta=0$). In addition, the absolute band gap, closed at $r=0.51a$ in the case without inclusion, opens up for values of β between 0.10 and 0.27. Improvement in the absolute PBG width is maximum for $\beta=0.15$ and $r=0.497a$ with a magnitude of $\Delta\omega/\omega_g=10\%$. This result is slightly different from the one in Ref. 8 because the dielectric contrast and computational method are different. The gap map for the optimum value of $\beta=0.15$ is shown in Fig. 2(b). As a result of the lifted degeneracy, the overlap between the two polarization gaps is extended. The absolute PBG is nearly three times larger than the best one for the basic square lattice. Although including an additional rod improves the absolute

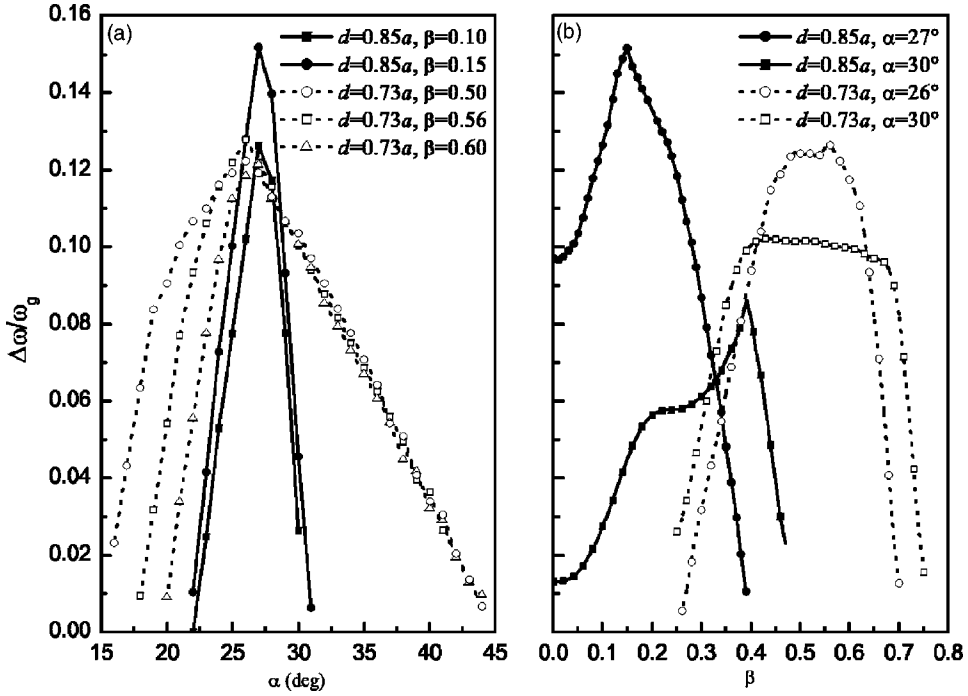

FIG. 6. Dependence of the absolute PBG width ($\Delta\omega/\omega_g$) on (a) the rotation angle α for fixed values of β and d/a; (b) the parameter $\beta=d'/d$ for fixed values of α and d/a for the modified square structure with included square rods [Fig. 1(f)]. The solid lines denote the width of the absolute PBG formed by the overlapping TE2-3 and TM3-4 polarization gaps. The dotted lines denote the width of the absolute PBG from the overlap by TE2-3 and TM4-5 polarization gaps.

PBG size, the fabrication of this structure becomes more difficult. The rod radius for the optimum absolute PBG nears the close-packed condition. Thus, for a gap centered at wavelength $\lambda=1.55$ μm the dielectric walls between adjacent holes should be 5 nm thick.

Next, a square structure of square rods and its corresponding modified structures designed by the inclusion of either square [Fig. 1(f)] or circular [Fig. 1(g)] air rods are considered. As mentioned before, the basic square structure of square rods does not exhibit an absolute PBG for any value of square length d. Band structure analysis indicates that the second and the third TE bands overlap, which prevents the TE2-3 gap from opening up. In addition, the third and fourth TM bands are degenerated at the Γ point of the Brillouin zone and no TM3-4 gap exists for values of $d<0.77a$. This band degeneracy can be lifted by rotating the square rods

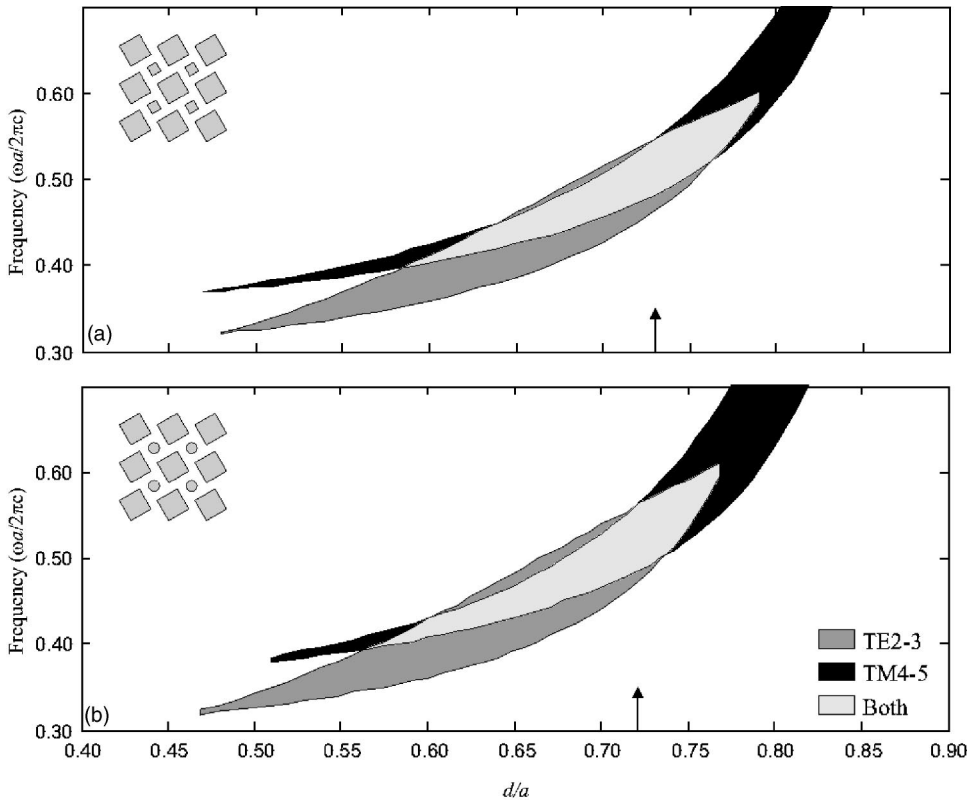

FIG. 7. Positions of TE2-3 and TM4-5 polarization gaps as functions of square length d/a for (a) a square structure with a square rod added at the center of the unit cell for $\beta=0.56$ and $\alpha=26°$ and (b) a square structure with a circular rod added at the center of the unit cell for $\beta=0.71$ and $\alpha=31°$. The picture insets show the structure under consideration. The positions of maximum absolute PBG width are indicated by arrows.

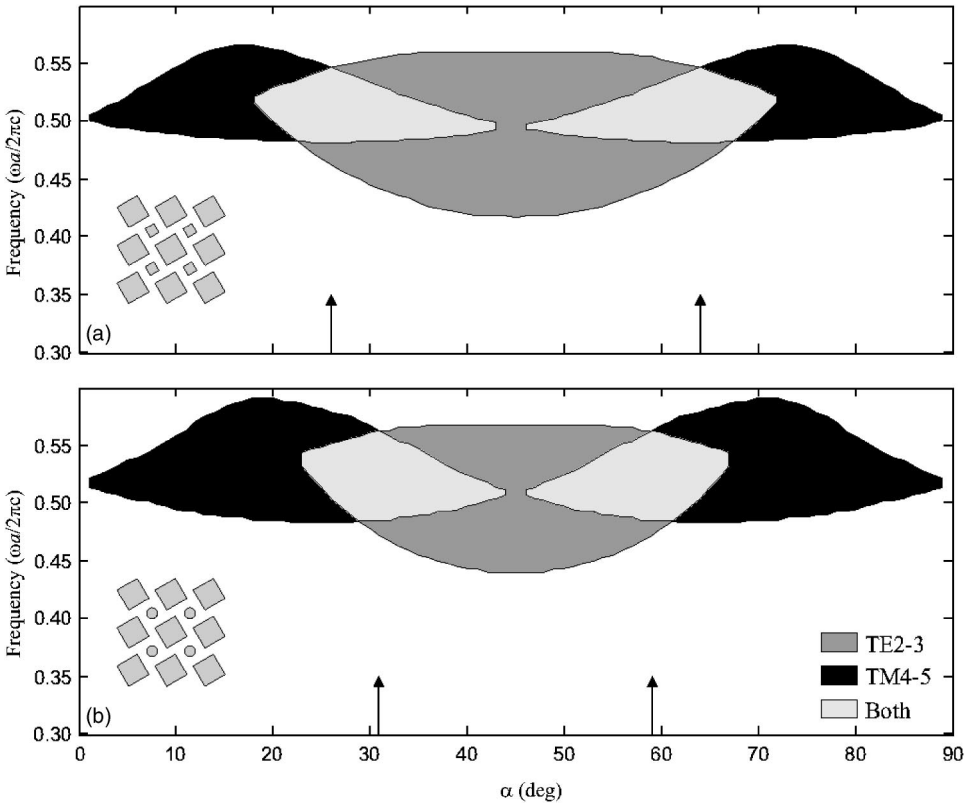

FIG. 8. Positions of TE2-3 and TM4-5 polarization gaps as functions of rotation angle α for (a) a square structure with a square rod added at the center of the unit cell for $\beta=0.56$ and $d=0.73a$ and (b) a square structure with a circular rod added at the center of the unit cell for $\beta=0.71$ and $d=0.72a$. The picture insets show the structure under consideration. The positions of maximum absolute PBG width are indicated by arrows.

with respect to the lattice axes. This, in turn, gives rise to an absolute PBG which results from the overlap between the TE2-3 and TM3-4 polarization gaps. To explain this, one can rely on the general rule of thumb.[1] The square lattice of square air rods is mainly a connected structure made up of high-index veins. The TE gaps are favored in connected structures, while the TM gaps are favored in structures of isolated high-index regions (spots). Rotating the square rods leads to a structure of isolated high-index spots that are linked by narrow veins. Suitable dielectric configurations for

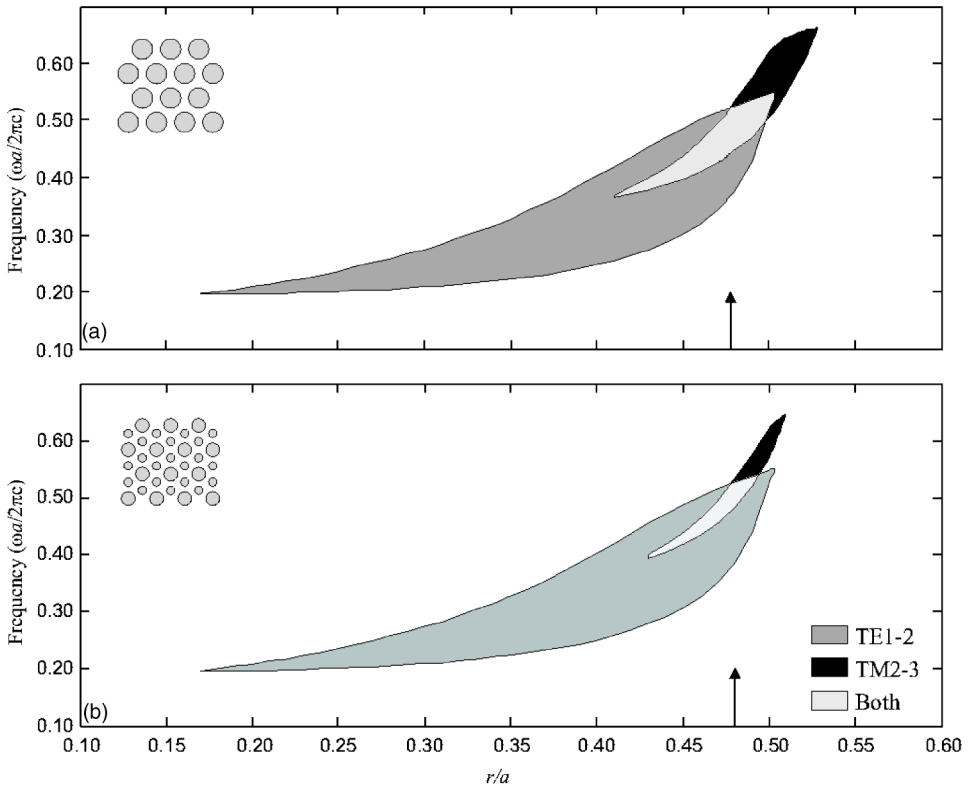

FIG. 9. Positions of TE1-2 and TM2-3 polarization gaps as functions of r/a for (a) basic triangular lattice of circular rods and (b) its modified structure with a circular rod added at the center of each triangle of the lattice unit cell for $\beta=0.1$. The positions of the maximum absolute PBG width are indicated by arrows.

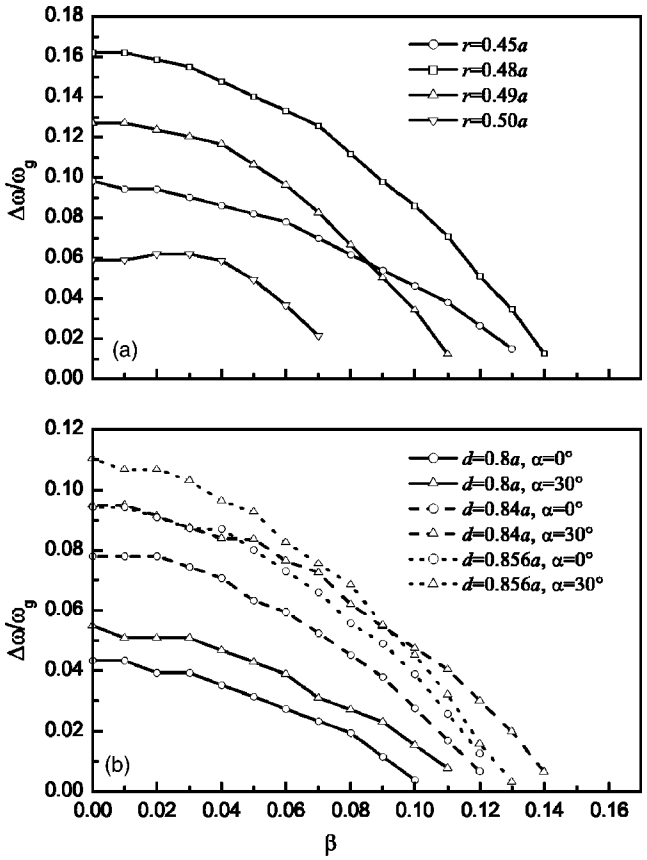

FIG. 10. Dependence of the absolute PBG width ($\Delta\omega/\omega_g$) on the parameter β for (a) the modified triangular structure of circular basic rods and a circular rod placed at the midpoint of each triangle formed of three basic rods and (b) a modified triangular structure of square basic rods and a circular rod placed at the midpoint of each triangle for different rotation angles.

opening an absolute PBG can therefore be formed.

Figure 4 shows the dependence of the absolute PBG width on the rotation angle α for different values of the square size d. The band gaps exhibit a symmetry with respect to rotation angle $\alpha=45°$ due to the inverse symmetry of the crystal. The absolute PBG reaches a maximum width of $\Delta\omega/\omega_g=13.8\%$ for $\alpha=32°$ and $d=0.806a$. This absolute PBG is roughly four times larger than the one for the basic square structure of circular air rods. In Fig. 5(a) the positions of the TE2-3 and TM3-4 polarization gaps are drawn as functions of the square length d. The closed-packed condition for rotation angle $\alpha=32°$ is $d_{cp}=0.848a$, so the smallest width of the narrow veins will be $0.050a$. For a gap centered at wavelength $\lambda=1.55\ \mu$m, the veins should be approximately 33 nm thick. This result is a more encouraging than the previous ones for the fabrication of photonic crystals.

Having discussed the square structure of rotated square rods, we now turn to the effects on photonic band gaps after an additional rod is included at the center of the lattice unit cell. For the modified square structure in Fig. 1(f) a square rod is added at the center of the unit cell, and for the modified lattice in Fig. 1(g) a circular rod is added. Besides the rotation angle α of the squares, a new degree of freedom is introduced into our calculations: a parameter β defined as the ratio between the lengths of the added d' and the basic rods d ($\beta=d'/d$) for the modified structure in Fig. 1(f), and the ratio between the diameter $2r'$ of the added rod and the length d of the basic rods ($\beta=2r'/d$) for the modified structure in Fig. 1(g). The size of the included rod is therefore related to the size of the basic rods in dimensionless units. First, we consider the modified structure with a square rod [Fig. 1(f)]. Numerical calculations for $\alpha=0°$ and different values of the parameter β have shown that there is no absolute PBG if the square rods are not rotated. Therefore, including an additional rod is not sufficient to open the absolute PBG for the given dielectric contrast. Figure 6(a) shows the dependence of the absolute PBG width on the rotation angle α for fixed values of the parameter β and the square length d and Fig. 6(b) shows the dependence of the absolute PBG width on the parameter β for fixed values of α and d. There is no easy way to find the optimum parametric environment (d,β,α) that maximizes the absolute PBG width. For instance, one can fix the rotation angle α and find the values of β and d which lead to the maximum width of the absolute PBG. The next step, logically, is to perform the calculations by fixing these values and varying α to find the optimum angle. However, this does not always lead to the optimum absolute PBG for the structure because, for the new optimum angle, there will be a new set of β and d. So, hard calculations are needed taking into account all possible values of α, β and d. From Fig. 6 we can see that absolute PBG width ($\Delta\omega/\omega_g=15.2\%$) is maximum when $\alpha=27°$, $\beta=0.15$ and $d=0.85a$. The positions of the TE2-3 and TM3-4 polarization gaps as functions of the square size d/a are drawn in Fig. 5(b). Including an additional rod does improve the absolute PBG width, but we also need to estimate the relative difficulty of fabrication for this improvement. For a rotation angle $\alpha=27°$, the close-packed condition is $d_{cp}=0.891a$. The size of the included rod is $d'=0.128a$ for $\beta=0.15$ and $d=0.85a$. The dielectric walls between adjacent basic rods will then have the smallest relative width of $0.046a$. For a gap centered at $\lambda=1.55\mu$m, the absolute width of the dielectric walls should be approximately 34 nm. Therefore, the fabrication of this structure is no more complicated than in the case without inclusion.

Our numerical calculations show that a new absolute PBG appears when the size of the included rod is increased. This is the result of overlapping between the TE2-3 and TM4-5 polarization gaps rather than the overlapping between the TE2-3 and TM3-4 gaps. Figure 6 shows the width of this absolute PBG as a function of rotation angle α and parameter β, respectively. We can see that the width of this absolute PBG is smaller than that of the absolute PBG formed by the overlapping of the TE2-3 and TM3-4 gaps. The main advantage, however, is that it extends over a wide range of square lengths d/a far away from the close-packed condition. This is a big advantage for the fabrication. For example, the maximum width of the absolute PBG formed by the overlapping of the TE2-3 and TM4-5 polarization gaps is $\Delta\omega/\omega_g=12.8\%$ when $\alpha=26°$, $\beta=0.56$ and $d=0.73a$. The close-packed condition for this angle is $d_{cp}=0.899a$. The included rod has a relative width of $d'=0.409a$. The relative width of the dielectric walls between adjacent basic rods is $0.188a$, but the thinnest elements, with a width of $0.099a$, are the

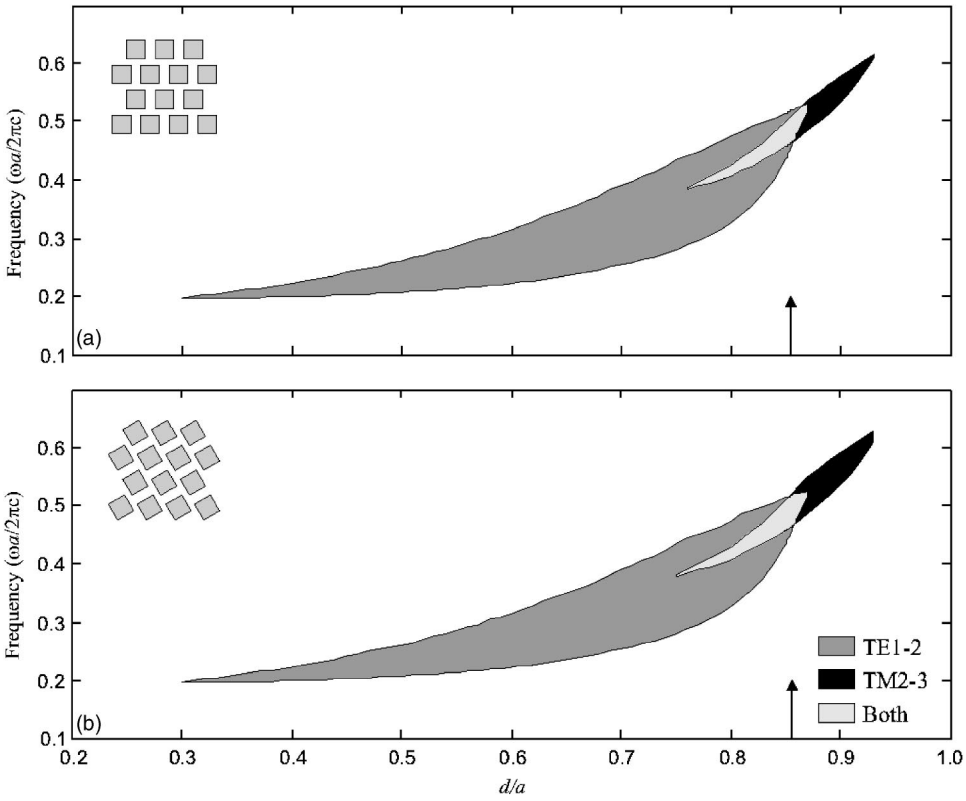

FIG. 11. Positions of TE1-2 and TM2-3 polarization gaps as functions of square size d/a for a triangular structure of square rods rotated at (a) $\alpha=0°$ and (b) $\alpha=30°$ with respect to the lattice axes. The positions of maximum absolute PBG are indicated by arrows.

walls between the basic and the included rods. For the gap centered at $\lambda=1.55$ μm, the absolute width should be approximately 79 nm. Figure 7(a) shows the positions of the TE2-3 and TM4-5 polarization gaps as functions of square length d/a. The absolute PBG exceeds 5% within $0.63<d/a<0.78$, which means that the smallest width of dielectric walls ranges between 117 and 54 nm. The angular dependence of the TE2-3 and TM4-5 gaps is shown in Fig. 8(a) for $d=0.73a$ and $\beta=0.56$. The absolute PBG exceeds 5% within $20°<\alpha<37°$. As a comparison, for these rotation angles the smallest width of dielectric walls would range between 57 and 67 nm. Although this is not the best absolute PBG for this structure, it seems to be better from the fabrication point of view.

Finally, we studied the modified square structure for which a circular rod is placed at the center of the lattice unit cell [Fig. 1(g)]. Our discussion is similar to that for the previous structure, so here we will only provide the main results. In this case, parameter β is defined as the ratio between the diameter $2r'$ of the included rod and the size d of the basic square rods. Figure 5(c) shows the positions of the TE2-3 and TM3-4 polarization gaps as functions of d/a. The optimum absolute PBG has a width of $\Delta\omega/\omega_g=15.6\%$ for $d=0.843a$, $\beta=0.15$ and $\alpha=28°$. For small values of β there is no significant difference between the modified structure with a circular rod included and the previously discussed structure with a square rod included. The size of the included rod is too small for $\beta=0.15$ so there is no significant change in the total filling fraction if the included rod is square or circular. This is not the case for values of $\beta>0.5$, which generate an absolute PBG from the overlapping between the TE2-3 and TM4-5 polarization gaps. Figures 7(b) and 8(b) show the positions of the TE2-3 and TM4-5 polarization gaps as functions of d/a for $\beta=0.71$, $\alpha=31°$ and as functions of α for $d=0.721a$, $\beta=0.71$, respectively. The maximum width of the absolute PBG is $\Delta\omega/\omega_g=14.8\%$, which is 2% greater than in the case of the interstitial lattice with a square rod included. For these physical parameters the smallest feature size is 57 nm. With this structure, therefore, we gain in absolute PBG width without harming the fabrication.

B. Triangular lattices

In this section we consider the triangular lattices of circular air rods [Fig. 1(c)] and square air rods [Fig. 1(d)] and their modified structures [Figs. 1(h) and 1(i)]. The triangular structure of circular air rods is known to present the greatest absolute PBG among the studied 2-D photonic crystals. The minimum refractive index contrast required for the opening of an absolute PBG is 2.66 for a filling fraction of the air rods of about 66%.[10] The absolute PBG is the result of the overlapping of the TE1-2 and TM2-3 polarizations gaps. Figure 9(a) shows the photonic band map for this structure. For the given dielectric contrast ($\varepsilon_{background}=12.096$ and $\varepsilon_{rod}=1$), the absolute PBG reaches a maximum width of $\Delta\omega/\omega_g=17\%$ for $r=0.478a$. The closed-packed condition for this structure is $r_{cp}=0.5a$. For the gap centered at $\lambda=1.55$ μm, the dielectric walls between adjacent rods must be 33 nm. This result is similar to that for the square lattices. We tried to apply the same approach i.e., to optimize the absolute PBG by reducing the lattice symmetry achieved either by inserting additional rods or by using noncircular scatterers.

First we studied the interstitial triangular structure [Fig. 1(h)] in which two additional rods are introduced into the

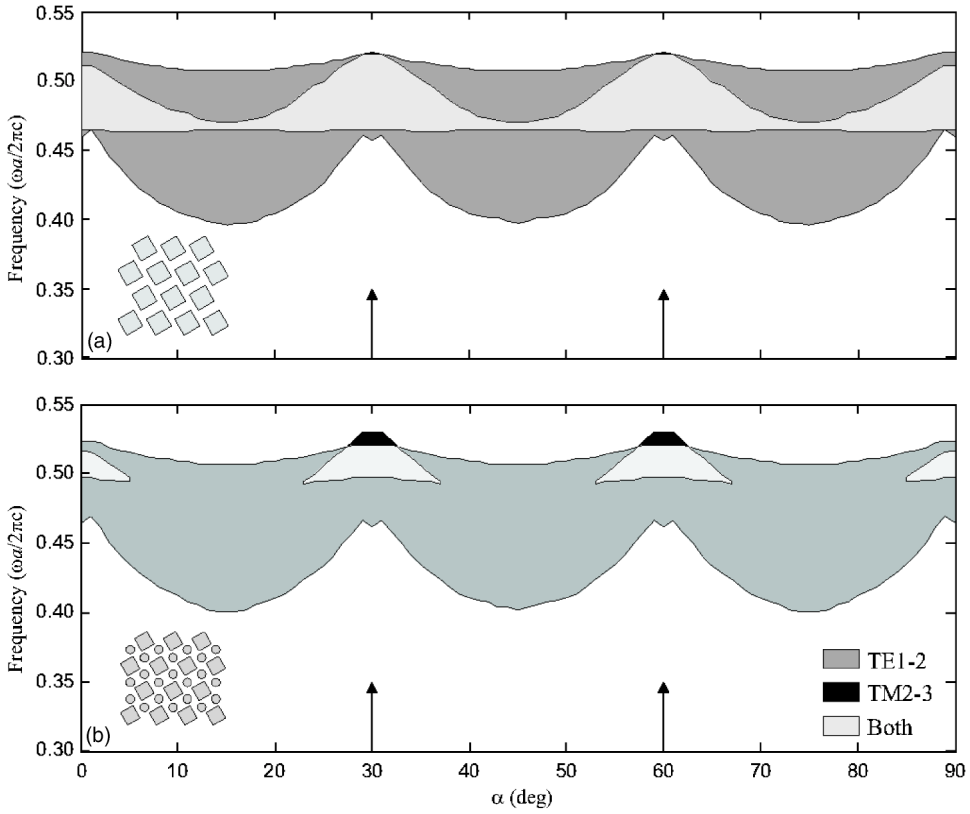

FIG. 12. Positions of TE1-2 and TM2-3 polarization gaps as functions of rotation angle α for (a) the basic triangular structure of square rods for $d=0.856a$ and (b) a modified triangular structure where two circular rods are introduced into the unit cell for $d=0.856a$ and $\beta=0.1$. The picture insets depict the structure under consideration. The positions of maximum absolute PBG width are indicated by arrows.

lattice unit cell. The included rods are located at the midpoint between three basic rods of the triangular lattice. For this structure the parameter $\beta=r'/r$ is defined as the ratio between the radii of included r' and basic r rods. The dependence of the absolute PBG width on the parameter β for some fixed values of the radius of basic rods r is shown in Fig. 10(a). For the case without inclusion ($\beta=0$), the structure switches to the basic triangular lattice of circular rods. Although the included rods are very small, their presence leads to a decrease in the absolute PBG width and, for values of β greater than 0.15, to complete closure of the gap. Figure 9(b) shows the positions of the TE1-2 and TM2-3 polarization gaps as functions of r/a for $\beta=0.1$. The maximum absolute PBG width is $\Delta\omega/\omega_g=8.6\%$ for $r=0.48a$. We can see that the TM2-3 polarization gap is strongly reduced. The inclusion of the interstitial air rods at the midpoint of each triangle disrupts the useful arrangement of the dielectric in isolated and linked regions. Isolated islands of high-index material do not yet exist. Therefore, TM gaps tend to disappear in such structures.

To continue our study on symmetry reduction we also examined the triangular lattice of square air rods [Fig. 1(d)]. Since the symmetry of the lattice is reduced, we must now consider all the directions of the new irreducible Brillouin zone, as shown in Fig. 1(l). For this structure there is an absolute PBG gap, which is result from the overlapping TE1-2 and TM2-3 polarization gaps, as in the case of the triangular structure of circular air rods. Their positions as functions of square size d/a are plotted in Fig. 11(a). The absolute PBG has a maximum width of $\Delta\omega/\omega_g=9.5\%$ for $d=0.854a$. The dielectric walls will have a relative width of $0.012a$ and should be about 9 nm thin for the gap centered at $\lambda=1.55$ μm. This structure therefore requires very stringent technological capabilities.

In the case of square structures, the rotation of square rods was an effective way to enlarge the absolute PBG. In the case of triangular lattices we go one step further and apply the same approach. Figure 12 plots the positions of the TE1-2 and TM2-3 polarization gaps as functions of the rotation angle α for a square size $d=0.856a$. Because of the mirror symmetries of the lattice, the gaps are symmetrical with respect to rotation angles α of 30° and 60°. Therefore, the only nonredundant rotations are those between 0° and 30°. The optimum rotation angle α, which provided the best improvement in the absolute PBG, was $\alpha=30°$. The positions of the TE1-2 and TM2-3 polarization gaps as functions of square size d/a are plotted in Fig. 11(b) for this optimum angle. The absolute PBG has a maximum width of $\Delta\omega/\omega_g=11\%$ for $d=0.856a$. If we bear in mind that the close-packed condition for $\alpha=30°$ is $d_{cp}=0.866a$, the relative width of the dielectric walls should be $0.010a$. For the gap centered at $\lambda=1.55$ μm, this results in an absolute width of approximately 8 nm. Rotating square rods in a triangular structure therefore does not, as it did in the case of square structures, significantly improve the absolute PBG.

By considering the modified triangular structure, which is formed by adding two circular rods in the unit cell [see Fig. 1(i)], we have studied the effects of symmetry reduction achieved both by rotating noncircular scatterers and including additional elements. As with the modified triangular lattice of circular rods, including additional rods considerably shrinks the absolute PBG. We found no improvement in the absolute PBG width for any rotation angle α of the square basic rods or for different values of β. Parameter β in this

TABLE I. Maximum normalized absolute PBG width for the considered structures. The table shows the physical parameters at which the optimum absolute PBG can be obtained. The relative and absolute sizes of the smallest element are also shown.

Lattice-scatterer	$\Delta\omega/\omega_g$	Physical parameters	Size of the smallest element	
			Relative	Absolute[a]
1. Square structures				
a. Square-circles	3.4%	$r=0.492a$	$0.016a$	10 nm
b. Square-circles with an additional circular rod	10%	$r=0.497a;\beta=0.15$	$0.006a$	5 nm
c. Square-squares		No absolute PBG exists		
d. Square-rotated squares	13.8%	$d=0.806a;\alpha=32°$	$0.050a$	33 nm
e. Square-rotated squares with an additional square rod	15.2%	$d=0.85a,\alpha=27°,\beta=0.15$[b]	$0.046a$	34 nm
	12.8%	$d=0.73a,\alpha=26°,\beta=0.56$[c]	$0.099a$	79 nm
f. Square-rotated squares with an additional circular rod	15.6%	$d=0.843a,\alpha=28°,\beta=0.15$[b]	$0.045a$	33 nm
	14.8%	$d=0.721a,\alpha=31°,\beta=0.71$[c]	$0.070a$	57 nm
2. Triangular structures				
a. Triangular-circles	17%	$r=0.478a$	$0.044a$	33 nm
b. Triangular-circles with two additional circular rods		There is no improvement in the absolute PBG size		
c. Triangular-squares	9.5%	$d=0.854a$	$0.012a$	9 nm
d. Triangular-rotated squares	11%	$d=0.856a;\alpha=30°$	$0.010a$	8 nm
e. Triangular-rotated squares with two additional circular rods		There is no improvement in the absolute PBG size		

[a]Absolute size for the gap centered at $\lambda=1.55$ μm.
[b]Absolute PBG formed from the overlapping TE2-3 and TM3-4 polarization gaps.
[c]Absolute PBG formed from the overlapping TE2-3 and TM4-5 polarization gaps.

case is defined as $\beta=2r'/d$ and relates the size of the included rods to the size of the basic rods. Moreover, again for values of β greater than 0.15 the absolute PBG completely disappears [Fig. 10(b)]. For triangular structures, therefore, symmetry reduction based on the inclusion of additional rods does not lead to a larger absolute PBG. The inclusion favorably increases the "air" filling fraction but disrupts the useful arrangement of high-index media in isolated and linked regions. From Fig. 12(b) we can see that, due to the inclusion, the TM2-3 polarization gap shrinks considerably, which decreases the absolute PBG width.

IV. SUMMARY AND CONCLUSIONS

We have performed a detailed numerical analysis of the photonic band structure of square and triangular lattices with circular and square rod profiles using the FDTD method. Specifically, we have examined how symmetry reduction, achieved by adding small rods to the lattice unit cell or by reorienting the square rods, affects the photonic band gap. Our results are summarized in Table I. For square lattices, the symmetry reduction approach has been successfully applied to maximize the absolute PBG width. For instance, in the case of a square lattice of circular rods, the inclusion of an additional rod leads to an absolute PBG, which is about three times larger than the one without inclusion. The rotation of the square rods is critical for opening the absolute PBG in the square structure of square rods. The most significant improvement in the size of the absolute PBG is provided by a combination of including an additional rod and rotating the square rods. Moreover, a new absolute PBG is generated that persists over a wide range of rotation angles and filling fractions far away from the closed-packed condition, and therefore greatly favors the fabrication of photonic crystals.

The largest absolute PBG is the one for the triangular structure of circular air rods. Our results show that modifying the crystal structure by adding interstitial rods or using square rods is not a good way to achieving larger absolute PBG, at least for the special case of air/silicon structures. Adding more rods in the lattice unit cell cannot further enlarge the absolute PBG width. Moreover, the absolute PBG shrinks dramatically because of disrupted islands of high-index material. Using square scatterers considerably reduces the absolute PBG width.

The dielectric walls of all these photonic crystals which are composed of air rods in a dielectric media should be extremely thin (Table I). To fabricate these crystals, we need highly developed technologies such as electron-beam lithography and dry-etching techniques. Such efforts are rewarded, however, by the large absolute PBG.

ACKNOWLEDGMENTS

The authors would like to thank Dr. Francisco Meseguer from Consejo Superior de Investigaciones Científicas (Unidad Asociada CSIC-UPV) for his critical reading of the manuscript and his helpful discussions. This work was supported by the Spanish Commission of Science and Technology (CICYT) under Grant No. TIC2002-04184-C02. It was also supported in part by the Supercomputing Center of Catalonia (CESCA), through an allocation of computer time.

*Corresponding author. Electronic address: lmarsal@etse.urv.es

[1] J. D. Joannopoulos, R. D. Meade, and J. N. Winn, *Photonic Crystals: Molding the Flow of Light* (Princeton University Press, Princeton, NJ, 1995).
[2] E. Yablonovitch, Phys. Rev. Lett. **58**, 2059 (1987).
[3] S. John and T. Quang, Phys. Rev. A **50**, 1764 (1994).
[4] E. Yablonovitch, T. J. Gmitter, R. D. Meade, A. M. Rappe, K. D. Brommer, and J. D. Joannopoulos, Phys. Rev. Lett. **B67**, 3380 (1991).
[5] S. L. McCall, P. M. Platzman, R. Dalichaouch, D. Smith, and S. Schultz, Phys. Rev. Lett. **67**, 2017 (1991).
[6] Z.-Y. Li, B.-Y. Gu, and G.-Z. Yang, Phys. Rev. Lett. **81**, 2574 (1998).
[7] D. Cassagne, C. Jouanin, and D. Bertho, Phys. Rev. B **53**, 7134 (1996).
[8] C. M. Anderson and K. P. Giapis, Phys. Rev. Lett. **77**, 2949 (1996).
[9] C. M. Anderson and K. P. Giapis, Phys. Rev. B **56**, 7313 (1997).
[10] P. R. Villeneuve and M. Piché, Phys. Rev. B **46**, 4969 (1992).
[11] M. Qiu and S. He, Phys. Rev. B **60**, 10610 (1990).
[12] R. Padjen, J. M. Gerard, and J. Y. Marzin, J. Mod. Opt. **41**, 295 (1994).
[13] X.-H. Wang, B.-Y. Gu, Z. Y. Li, and G.-Z. Yang, Phys. Rev. B **60**, 11417 (1999).
[14] L. F. Marsal, T. Trifonov, A. Rodríguez, J. Pallarès, and R. Alcubilla, Physica E (Amsterdam) **16**, 580 (2003).
[15] J. D. Joannopoulos, P. R. Villeneuve, and F. Shanhui, Nature (London) **386**, 143 (1997).
[16] C. T. Chan, Q. L. Yu, and K. M. Ho, Phys. Rev. B **51**, 16635 (1995).
[17] K. Sakoda, *Optical Properties of Photonic Crystals* (Springer-Verlag, Germany, 2001)
[18] P. R. Villeneuve and M. Piché, Phys. Rev. B **46**, 4973 (1992).